



**AALBORG UNIVERSITY**  
DENMARK

**Aalborg Universitet**

## **Hysteresis nonlinearity modeling and linearization approach for Envelope Tracking Power Amplifiers in wireless systems**

Al-kanan, Haider; Tafuri, Felice; Li, Fu

*Published in:*  
Microelectronics Journal

*DOI (link to publication from Publisher):*  
[10.1016/j.mejo.2018.10.006](https://doi.org/10.1016/j.mejo.2018.10.006)

*Creative Commons License*  
CC BY-NC-ND 4.0

*Publication date:*  
2018

*Document Version*  
Accepted author manuscript, peer reviewed version

[Link to publication from Aalborg University](#)

*Citation for published version (APA):*  
Al-kanan, H., Tafuri, F., & Li, F. (2018). Hysteresis nonlinearity modeling and linearization approach for Envelope Tracking Power Amplifiers in wireless systems. *Microelectronics Journal*, 82, 101-107.  
<https://doi.org/10.1016/j.mejo.2018.10.006>

### **General rights**

Copyright and moral rights for the publications made accessible in the public portal are retained by the authors and/or other copyright owners and it is a condition of accessing publications that users recognise and abide by the legal requirements associated with these rights.

- ? Users may download and print one copy of any publication from the public portal for the purpose of private study or research.
- ? You may not further distribute the material or use it for any profit-making activity or commercial gain
- ? You may freely distribute the URL identifying the publication in the public portal ?

### **Take down policy**

If you believe that this document breaches copyright please contact us at [vbn@aub.aau.dk](mailto:vbn@aub.aau.dk) providing details, and we will remove access to the work immediately and investigate your claim.

# Accepted Manuscript

Hysteresis nonlinearity modeling and linearization approach for Envelope Tracking Power Amplifiers in wireless systems

Haider Al-kanan, Felice Tafuri, Fu Li



PII: S0026-2692(18)30400-2

DOI: <https://doi.org/10.1016/j.mejo.2018.10.006>

Reference: MEJ 4430

To appear in: *Microelectronics Journal*

Received Date: 31 May 2018

Revised Date: 31 August 2018

Accepted Date: 14 October 2018

Please cite this article as: H. Al-kanan, F. Tafuri, F. Li, Hysteresis nonlinearity modeling and linearization approach for Envelope Tracking Power Amplifiers in wireless systems, *Microelectronics Journal* (2018), doi: <https://doi.org/10.1016/j.mejo.2018.10.006>.

This is a PDF file of an unedited manuscript that has been accepted for publication. As a service to our customers we are providing this early version of the manuscript. The manuscript will undergo copyediting, typesetting, and review of the resulting proof before it is published in its final form. Please note that during the production process errors may be discovered which could affect the content, and all legal disclaimers that apply to the journal pertain.

# Hysteresis Nonlinearity Modeling and Linearization Approach for Envelope Tracking Power Amplifiers in Wireless Systems

Haider Al-kanan<sup>1\*</sup>, Felice Tafuri<sup>2</sup>, Fu Li<sup>1</sup>

<sup>1</sup> Department of Electrical and Computer Engineering, Portland State University, Portland, Oregon, USA

<sup>2</sup> Department of Electronic Systems, Aalborg University, Aalborg, Denmark

\*E-mail: haider2@pdx.edu

**Abstract:** Novel Dual-Input Single-Output (DISO) behavioral modeling and linearization techniques for Envelope Tracking Power Amplifiers (ET PAs) in wireless application are presented in this paper. The proposed modeling approach applies the Hammerstein structure for the Amplitude-to-Phase (AM/PM) conversion. An extension of the Saleh AM/PM model is also proposed to model the static nonlinearity in the ET PA AM/PM conversion. This paper presents a new linearization technique for ET PAs by inverting the proposed ET PA model and using it as a Digital Predistortion (DPD). The measurement results show that both the proposed model and DPD can clearly outperform both the original Saleh model and the DPD based on the Saleh model inversion. Compared to the state-of-the-art behavioral models for ET PAs, the proposed model and DPD can offer an improved complexity-accuracy trade-off thanks to the lower number of coefficients.

Keywords: Envelope tracking, hysteresis effects, linearization, nonlinearity, power amplifiers.

## 1. Introduction

Envelope Tracking (ET) is a technique that has been widely deployed in RF Power Amplifiers (PAs) to enhance the power efficiency in wireless communications (i.e 4G). The wide bandwidth and high Peak-to-Average Power Ratio (PAPR) of the modern wireless waveforms (i.e 4G/5G) pose significant challenges to the ET PA design [1]–[2]. Power amplifiers produce significant hysteresis nonlinearity when operated at high PAPR and wide bandwidth signals because of the wide dynamic variation in the transistor parasitic capacitance and inductance. In addition, the biasing and matching circuits in PAs are frequency-dependent components. The hysteresis effects can have long-time constants in both amplitude and phase of the baseband signals. Hence, it is difficult to accurately predict the circuit response. The dynamic supply voltage in envelope tracking scenario can also affect the PA circuit characteristics [3]. Various behavioral models have been presented in the literature to characterize the hysteresis nonlinearity in ET PA for different accuracy and model complexity [2]–[8]. The mathematical models using two-dimensional look-up tables are simpler approaches for the ET PA modeling. However, they have low accuracy because they are implemented based on the data interpolation approximation [4]. Single-Input Single-Output (SISO) and Dual-Input Single-Output (DISO) memory models derived from Volterra series (i.e Generalized Memory Polynomial Model (GMPM)) have been widely deployed for ET PA modeling and linearization. However, these models often require a high number of coefficients, which can increase the numerical operations instability in such ways as inverting matrices of a large number of elements when estimating the model coefficients. In addition, the computational expensive model makes the real time implementation of the DPD more difficult. Another drawback of a complex model architecture is that it can be mathematically difficult to invert it (i.e Cann

model [8]) for DPD identification.

This paper presents a low complexity and high accuracy behavioral model for ET PA and novel linearization techniques. The proposed extension of the Saleh Amplitude-to-Phase (AM/PM) model and the Hammerstein approach are important techniques that improve the model's accuracy and reduce its complexity. The dynamic supply voltage is considered in the AM/PM model to account for the change in the PA characteristics due to the dynamic supply voltage in the envelope tracking scenario. The proposed ET PA modeling approach can predict the dynamic nonlinearity in the Amplitude-to-Amplitude (AM/AM) and AM/PM conversions due to the hysteresis effects of the energy storage elements in power amplifier circuits. This paper also describes the inversion techniques of the DISO ET PA model when identifying the DPD to linearize both the AM/AM and AM/PM conversions. The proposed DPD model can linearize the distortion contributions induced by the modulated supply voltage.

This paper is organized as follows: Section 2 describes the proposed model structure and the AM/PM extension of the Saleh behavioral model. Section 3 presents the derivation of the proposed DISO DPD model to compensate for the nonlinear distortion in the ET PA. Section 4 describes the experimental results, including the measurement set-up, and the performance evaluation of the proposed model and linearization techniques. Finally, Section 5 outlines the conclusions.

## 2. Proposed ET PA Model

The ET PA system can be represented in a simplified block diagram using an equivalent baseband DISO structure as shown in Fig. 1. The DISO behavioral model is a black-box representation which describes the two-to-one relationship

of the PA ports. The ET PA model output can be mathematically expressed in terms of AM/AM and AM/PM functions using the complex notation in magnitude and phase as

$$z = f_A(r, v_s) e^{j(f_p(r, v_s) + \angle x)} \quad (1)$$

where  $f_A(\cdot)$  and  $f_p(\cdot)$  are the ET PA AM/AM and AM/PM functions, respectively.  $r$  is the magnitude of the complex baseband input signal  $x$  which consists of In-phase (I) and Quadrature-phase (Q) components.  $v_s$  is the PA modulated supply voltage,  $z$  is the corresponding complex baseband output of the ET PA. The operator  $\angle(\cdot)$  is used to indicate the phase of the complex variable. The output of the  $f_A(\cdot)$ , and  $f_p(\cdot)$  functions are represented by  $y_d$  and  $\theta_d$ , respectively. The  $f_A(\cdot)$  function was modeled using a static AM/AM function in (2) in cascade with a Finite Impulse Response (FIR) filter in (3) as in [5].

$$y(r, v_s) = \frac{r \sum_{i=1}^{N_A} \alpha_i v_s^i}{1 + r^2 \sum_{j=1}^{N_B} \beta_j v_s^j} \quad (2)$$

where  $y(r, v_s)$  is the output magnitude of the extended Saleh AM/AM model,  $\alpha_i$  and  $\beta_j$  are Saleh model coefficients, and  $N_A$  and  $N_B$  are the maximum orders of the polynomial functions in  $\alpha_i$  and  $\beta_j$ , respectively. The memory effects in the AM/AM conversion were considered as in [5] using the FIR filter as

$$y_d(n) = \sum_{m=0}^{M_{AM}} h(m) y(n-m) \quad (3)$$

where  $h(m)$  represents the filter coefficients,  $M_{AM}$  is the memory depth in the AM/AM conversion, and  $y_d(n)$  is the output of the dynamic AM/AM model.

In this paper, we propose to model the dynamic AM/PM conversion using the Hammerstein approach. Hammerstein provides a simpler and more flexible way for modeling the dynamic nonlinear systems [9]. The dynamic AM/PM conversion is modeled using a static DISO model (Saleh AM/PM extension) in series with the FIR filter to account for the hysteresis effects in the AM/PM conversion. The

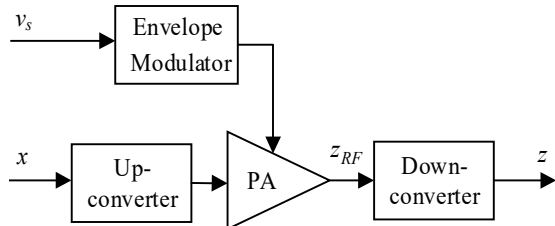


**Fig. 1.** Block diagram of the equivalent baseband DISO representation of the ET PA.

model architecture of the dynamic AM/AM and AM/PM components is depicted in Fig. 2.

### 2.1 Proposed Saleh AM/PM Extension

The Saleh AM/PM model [10] for constant-supply PA can be expressed as

$$\theta = \frac{r^2 \lambda}{1 + r^2 \gamma} \quad (4)$$

where  $\lambda$  and  $\gamma$  are the Saleh AM/PM model parameters, and  $\theta$  is the output phase. The ET PA phase is dynamically varying with the supply voltage [11]. Hence, we propose to express the parameters of the Saleh AM/PM conversion as polynomial functions of the modulated supply voltage as

$$\theta(r, v_s) = \frac{r^2 \lambda(v_s)}{1 + r^2 \gamma(v_s)} \quad (5)$$

where  $\lambda(v_s)$  and  $\gamma(v_s)$  are proposed to model as follows:

$$\lambda(v_s) = \sum_{i=1}^{P_a} \lambda_i v_s^i \quad (6)$$

$$\gamma(v_s) = \sum_{i=1}^{P_b} \gamma_i v_s^i \quad (7)$$

The  $P_a$  and  $P_b$  are the maximum orders of the polynomial functions. By substituting (6) and (7) in (5), we obtain a static DISO Saleh AM/PM function which can be expressed as

$$\theta(r, v_s) = \frac{r^2 \sum_{j=1}^{P_a} \lambda_j v_s^j}{1 + r^2 \sum_{j=1}^{P_b} \gamma_j v_s^j} \quad (8)$$

The polynomial functions in (8) can be expressed in a vector form as

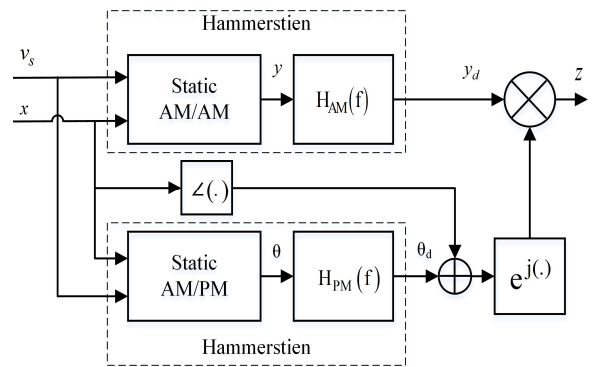


**Fig. 2.** Block diagram of the proposed ET PA model architecture.

$$\theta = \frac{r^2 \lambda \mathbf{v}_\lambda^T}{1 + r^2 \gamma \mathbf{v}_\gamma^T} \quad (9)$$

where  $\lambda = [\lambda_1 \lambda_2 \dots \lambda_{P_a}]$  and  $\gamma = [\gamma_1 \gamma_2 \dots \gamma_{P_b}]$  are the model coefficients, and  $\mathbf{v}_\lambda$  and  $\mathbf{v}_\gamma$  are vectors of the modulated supply voltage in the polynomial orders as

$$\mathbf{v}_\lambda = [v_s^1 \ v_s^2 \ \dots \ v_s^{P_a}] \quad (10)$$

$$\mathbf{v}_\gamma = [v_s^1 \ v_s^2 \ \dots \ v_s^{P_b}] \quad (11)$$

### 2.1.1 Coefficients Estimation

The extended AM/PM model in (9) can be expressed as

$$\theta = r^2 \lambda \mathbf{v}_\lambda^T - \theta r^2 \gamma \mathbf{v}_\gamma^T \quad (12)$$

By applying the time samples on (12), we obtain the following matrix equation:

$$\begin{bmatrix} \theta(1) \\ \theta(2) \\ \vdots \\ \vdots \\ \vdots \\ \theta(k) \end{bmatrix} = \begin{bmatrix} r(1)^2 \mathbf{v}_\lambda[1] & -\theta(1)r(1)^2 \mathbf{v}_\gamma[1] \\ r(2)^2 \mathbf{v}_\lambda[2] & -\theta(2)r(2)^2 \mathbf{v}_\gamma[2] \\ \vdots & \vdots \\ \vdots & \vdots \\ \vdots & \vdots \\ r(k)^2 \mathbf{v}_\lambda[k] & -\theta(k)r(k)^2 \mathbf{v}_\gamma[k] \end{bmatrix} \begin{bmatrix} \lambda_1 \\ \vdots \\ \lambda_{P_a} \\ \gamma_1 \\ \vdots \\ \gamma_{P_b} \end{bmatrix} \quad (13)$$

where  $k$  is the time sample, and  $\mathbf{v}_\lambda$  and  $\mathbf{v}_\gamma$  are the row vectors that are expressed as

$$\mathbf{v}_\lambda[k] = [v_s^1(k) \ v_s^2(k) \ \dots \ v_s^{P_a}(k)] \quad (14)$$

$$\mathbf{v}_\gamma[k] = [v_s^1(k) \ v_s^2(k) \ \dots \ v_s^{P_b}(k)] \quad (15)$$

Equation (13) can be expressed in a matrix notation as

$$\boldsymbol{\theta} = \mathbf{Q} \mathbf{L} \quad (16)$$

where  $\boldsymbol{\theta}$  is a  $(k \times 1)$  column vector of the ET PA output phase samples,  $\mathbf{Q}$  is a  $(k \times (P_a + P_b))$  matrix includes the samples of the baseband input magnitude and modulated supply voltage, and  $\mathbf{L}$  is a  $((P_a + P_b) \times 1)$  vector of the model coefficients. The model coefficients  $\mathbf{L}$  can be calculated as

$$\mathbf{L} = (\mathbf{Q})^\dagger \boldsymbol{\theta} \quad (17)$$

where  $(\cdot)^\dagger$  denotes the matrix pseudo-inverse which can be calculated using the Least Squares (LS) as

$$\mathbf{Q}^\dagger = (\mathbf{Q}^T \mathbf{Q})^{-1} \mathbf{Q}^T \quad (18)$$

where  $(\cdot)^T$  denotes the matrix transpose.

## 2.2 Hysteresis Effects

The energy storage elements in the power amplifier circuits (i.e capacitors and inductors) cause hysteresis (or memory) effects in both AM/AM and AM/PM nonlinearities. Other causes of hysteresis effects include the dynamic variation of the amplifier chip temperature [12]. The PA operation under time-varying supply voltage in the ET scenario can also cause an additional hysteresis effect in the AM/PM conversion [6], [13]. We use the FIR filter in cascade with the static AM/PM nonlinear model in order to consider the hysteresis behavior in the AM/PM nonlinearity. In other words, the FIR filter is used to model the residuals that are not possible to capture using the static model in (9) due to the memory effects. The dynamic output phase  $\theta_d(n)$  of the complete AM/PM model can be expressed as

$$\theta_d(n) = \sum_{m=0}^{M_{PM}} g(m) \theta(n-m) \quad (19)$$

where  $M_{PM}$  is the memory depth of the proposed AM/PM model,  $\theta$  is the output phase of the static model in (9), and  $g(m)$  represents the filter coefficients. A least squares method can be used to calculate the FIR filter coefficients as

$$\mathbf{g} = (\boldsymbol{\Psi}^T \boldsymbol{\Psi})^{-1} \boldsymbol{\Psi}^T \boldsymbol{\theta}_d \quad (20)$$

where  $\mathbf{g}$  is a vector of the FIR filter coefficients,  $\boldsymbol{\theta}_d$  is a vector of the output phase samples  $\theta_d(n)$ , and  $\boldsymbol{\Psi}$  is a matrix composed from the extended Saleh model output phase samples  $\theta(n)$ .

The total number of coefficients ( $N_c$ ) for the complete proposed model is

$$N_c = N_A + N_B + P_a + P_b + M_{PM} + M_{AM} + 2 \quad (21)$$

## 3. Proposed Digital Predistortion

An important property of the Saleh model for the constant-supply voltage is that it can be mathematically inverted to obtain a digital predistortion [14]-[15]. The modulated supply voltage  $v_s$  is considered a new independent variable in a DISO DPD modeling scenario to account for the nonlinear distortion due to the dynamic variation of the supply voltage [4], [6], [13], [11]. This section presents the DPD model which consists of two functions, the AM/AM DPD function which is used to linearize the PA gain, and the AM/PM DPD function which is used to linearize the PA phase. The inversion approach of each DISO function is presented as follows:

### 3.1 AM/AM Digital Predistortion

The AM/AM digital predistortion is a nonlinear function combined to the ET PA AM/AM function to produce a

linear power gain. The AM/AM DPD can be expressed as an inverse function of the proposed ET AM/AM model as

$$D_A(u, v_s) = y^{-1}(r, v_s) \quad (22)$$

The  $D_A(\cdot)$  is the DPD AM/AM function, and  $y(\cdot)$  is the ET PA static AM/AM function defined in (2). The polynomial functions in (2) can be expressed in a vector form to simplify the derivations as

$$y(r, v_s) = \frac{\boldsymbol{\alpha} \mathbf{v}_\alpha^T r}{1 + \boldsymbol{\beta} \mathbf{v}_\beta^T r^2} \quad (23)$$

where  $\boldsymbol{\alpha} = [\alpha_1 \ \alpha_2 \ \dots \ \alpha_{N_A}]$  and  $\boldsymbol{\beta} = [\beta_1 \ \beta_2 \ \dots \ \beta_{N_B}]$  are vectors of the ET PA model coefficients, and  $\mathbf{v}_\alpha$  and  $\mathbf{v}_\beta$  are vectors defined as

$$\mathbf{v}_\alpha = [v_s^1 \ v_s^2 \ \dots \ v_s^{N_A}] \quad (24)$$

$$\mathbf{v}_\beta = [v_s^1 \ v_s^2 \ \dots \ v_s^{N_B}] \quad (25)$$

The DPD model output is the same as the ET PA input, because they are connected in series as shown in Fig. 3. Hence, the output of the AM/AM DPD model is

$$D_A(q, v_s) = r \quad (26)$$

where  $q$  is introduced to represent the magnitude of the DPD complex baseband input signal  $u$ , and  $r$  is the magnitude of the ET PA baseband input signal  $x$ . The objective of the  $D_A(\cdot)$  function is to compensate for the static AM/AM nonlinear distortion. Therefore, the condition to be satisfied by a linearized ET PA AM/AM can be expressed as

$$y(D_A(q, v_s)) = q \quad (27)$$

Substituting (23) and (26) into (27) leads to

$$\frac{\boldsymbol{\alpha} \mathbf{v}_\alpha^T r}{1 + \boldsymbol{\beta} \mathbf{v}_\beta^T r^2} = q \quad (28)$$

Equation (28) can be rewritten in a quadratic formula as

$$\boldsymbol{\beta} \mathbf{v}_\beta^T q r^2 - \boldsymbol{\alpha} \mathbf{v}_\alpha^T r + q = 0 \quad (29)$$

The solution of (29) can be calculated as

$$r = \frac{\boldsymbol{\alpha} \mathbf{v}_\alpha^T - \sqrt{(\boldsymbol{\alpha} \mathbf{v}_\alpha^T)^2 - 4 \boldsymbol{\beta} \mathbf{v}_\beta^T q^2}}{2 \boldsymbol{\beta} \mathbf{v}_\beta^T q} \quad (30)$$

A negative sign solution is considered in the square root,

because the variable  $r$  is real and normalized in this work. Equation (29) is valid within the magnitude interval defined as

$$0 \leq q \leq \sqrt{\frac{(\boldsymbol{\alpha} \mathbf{v}_\alpha^T)^2}{4 \boldsymbol{\beta} \mathbf{v}_\beta^T}} \quad (31)$$

The AM/AM DPD function in (30) considers the nonlinearity due to the modulated supply voltage represented by the polynomial vectors  $\mathbf{v}_\alpha$  and  $\mathbf{v}_\beta$ . This is an additional advantage for improving the linearization capability.

### 3.2. AM/PM Digital Predistortion

The AM/PM DPD function  $D_P(\cdot)$  is introduced to eliminate the AM/PM distortion of the ET PA. Thus, the objective of the AM/PM DPD function is to cancel out the ET PA AM/PM conversion as

$$e^{j(D_P(q, v_s))} \cdot e^{j(\theta(r, v_s))} = 1 \quad (32)$$

where  $\theta(\cdot)$  is the ET PA AM/PM function which was derived in Section 2.1. The  $D_P(\cdot)$  function can be calculated by substituting (9) into (32) as

$$D_P(q, v_s) = \frac{-q^2 \boldsymbol{\lambda} \mathbf{v}_\lambda^T}{1 + q^2 \boldsymbol{\gamma} \mathbf{v}_\gamma^T} \quad (33)$$

where  $\boldsymbol{\lambda}$  and  $\boldsymbol{\gamma}$  are the ET PA coefficient vectors which were derived in Section 2.1.1. The complex representation of the complete DPD model can be expressed in terms of the AM/AM function  $D_A(\cdot)$  and the AM/PM function  $D_P(\cdot)$  as

$$x = D_A(q, v_s) e^{j(D_P(q, v_s) + \angle u)} \quad (34)$$

A block diagram of the complete DPD architecture with ET PA is shown in Fig. 3. The derived AM/AM and AM/PM DPD expressions in (30) and (33) are simple as compared to the state-of-the-art DPD model. In addition, the proposed DPD model uses the same coefficients of the proposed ET PA model. This is another advantage that can significantly reduce the computational cost for the DPD coefficient's identification.

## 4. Experimental Results

### 4.1 Experimental Set-up

The data acquisition and validation system for the envelope tracking power amplifier was implemented as shown in Fig. 4. The measurement set-up consists of a RF signal generator which was connected to the RF power amplifier, and a

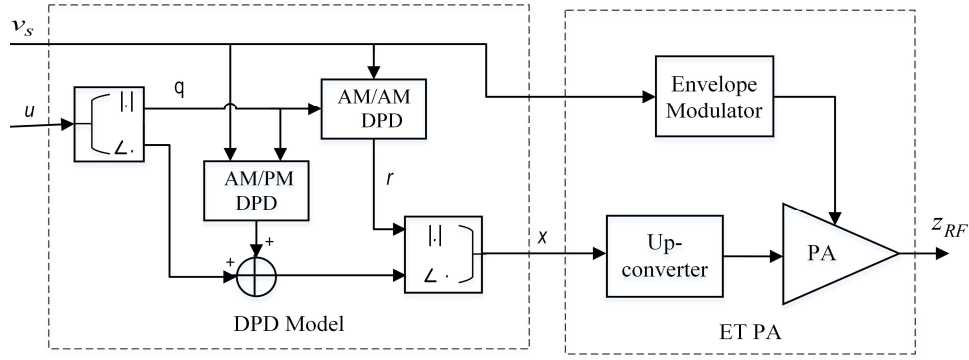


Fig. 3. Block diagram of the proposed DPD model structure.

waveform generator which was connected to the envelope modulator. Both the RF signal generator and the waveform generator were controlled by MATLAB software.

The ET PA was designed using a RF power amplifier (RFPA3809) from RFMD and an in-house linear envelope modulator designed using OPA2674 from Texas Instruments. The ET PA system was driven by 10,000 symbols of 3.84 MHz bandwidth WCDMA signal. A DC power supply was used to feed the main power amplifier and the envelope modulator.

The power amplifier output signal was acquired using the signal analyzer and exported to MATLAB in a complex baseband format for modeling computations and accuracy evaluation.

#### 4.2 Behavioral Modeling Results

The proposed model coefficients were calculated based on the obtained data from the experiment, and for the model nonlinear orders  $N_A=3$ ,  $N_B=2$ ,  $P_a=2$ , and  $P_b=3$ . The proposed model results as well as the measured results of

gain and phase conversions are depicted in Fig. 5. This shows a significant modeling improvement in both AM/AM and AM/PM conversions as compared to the original Saleh model. The modeling accuracy was evaluated in the time domain using Normalized Mean Square Error (NMSE) and in the frequency domain using Adjacent Channel Error Power Ratio (ACEPR). NMSE and ACEPR are figures of merit that are widely used in the state-of-the-art model accuracy evaluation [5]–[8] and they are defined, respectively as follows [16]:

$$NMSE = 10 \log_{10} \left( \frac{\sum_{n=1}^J |z_s(n) - z_m(n)|^2}{\sum_{n=1}^J |z_s(n)|^2} \right) \quad (35)$$

where  $z_s(n)$  and  $z_m(n)$  are the baseband output measured and modeled signals, respectively.  $J$  is the total number of symbols.

$$ACEPR = 10 \log_{10} \left( \frac{\int_{f_{s,L}}^{f_{p,L}} |E(f)|^2 df + \int_{f_{s,U}}^{f_{p,U}} |E(f)|^2 df}{\int_{f_{s,ch}}^{f_{p,ch}} |Z_s(f)|^2 df} \right) \quad (36)$$

where  $E(f)$  is the frequency domain error signal ( $z_s - z_m$ ),  $Z_s(f)$  is the frequency domain of the measured ET PA output signal.  $f_{s,L}$  and  $f_{p,L}$  are the start and stop frequencies, respectively, of the lower adjacent channel.  $f_{s,U}$  and  $f_{p,U}$  are the start and stop frequencies, respectively, of the upper adjacent channel.  $f_{s,ch}$  and  $f_{p,ch}$  are the start and stop frequencies, respectively, of the desired channel. The proposed modeling NMSE versus the swept maximum nonlinear orders  $N_A$ ,  $N_B$ ,  $P_a$ , and  $P_b$  are depicted in Fig. 6. This indicates the optimal static model accuracy. The amount of the memory depth in the AM/AM and AM/PM

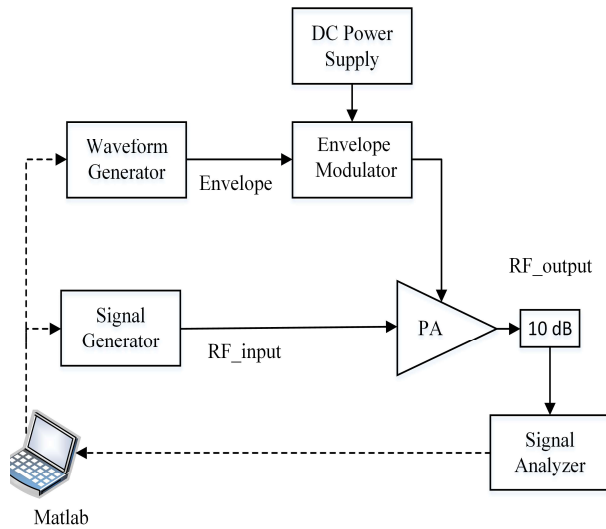
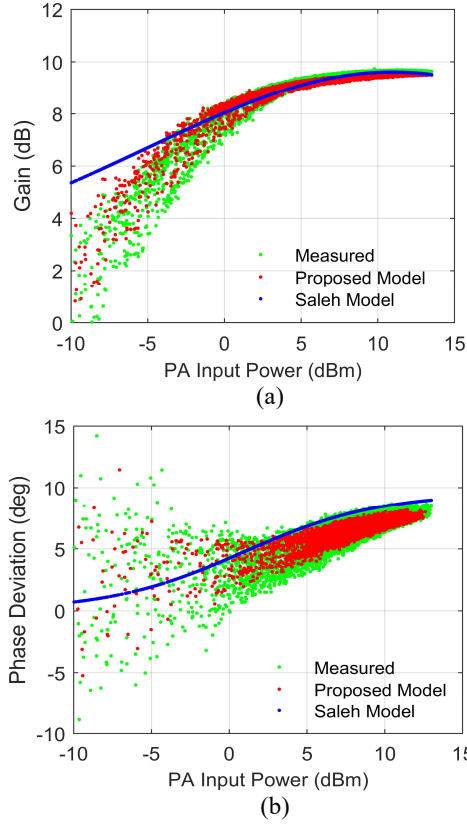


Fig. 4. Block diagram of the experimental set-up.

conversions can be obtained from the model NMSE versus the swept memory depth  $M_{AM}$  and  $M_{PM}$  as shown in Fig. 7. The proposed model accuracy evaluation is compared to the state-of-the-art ET PA models, such as the Dual-Input Memory Polynomial Model (2D-MPM) and the Memory Binomial Model (MBM) [6], each for a different number of coefficients.

The compared behavioral modeling accuracy for different nonlinear orders and memory depth is shown in Table 1. The NMSE and ACEPR -42.48 dB and -51.80 dB, respectively, are the optimal model accuracy compared to the optimal performance of the 2D-MPM and MBM as shown in Fig. 8.



**Fig. 5.** Measured and modeled results. (a) Gain. (b) Phase deviation.

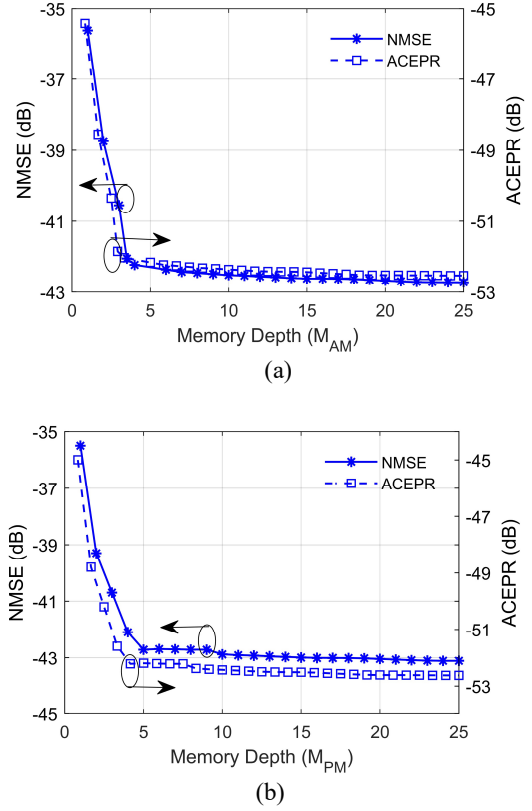


**Fig. 7.** NMSE and ACEPR versus the swept memory depth. (a) NMSE and ACEPR versus the memory depth  $M_{AM}$ , where  $M_{PM}$  is set to 5. (b) NMSE and ACEPR versus the memory depth  $M_{PM}$ , where  $M_{AM}$  is set to 5.

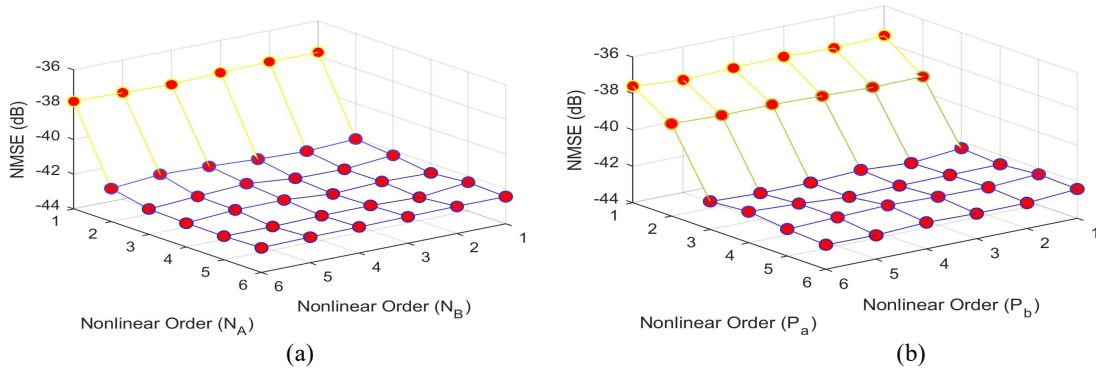


**Fig. 6.** NMSE versus the model maximum nonlinear orders. (a) NMSE versus  $N_A$  and  $N_B$ . (b) NMSE versus  $P_a$  and  $P_b$ .



**Table 1** Models' NMSE and ACEPR versus the number of coefficients

Model	Number of Coefficients	Nonlinear Order	Memory Depth	NMSE(dB)	ACEPR(dB)
Proposed	12	$N_A=2, N_B=1, P_a=2, P_b=1$	$M_{AM}=2, M_{PM}=2$	-38.32	-47.62
	20	$N_A=3, N_B=2, P_a=2, P_b=3$	$M_{AM}=4, M_{PM}=4$	-42.48	-51.80
Dual-Input Memory Polynomial	27	$K=2, N=3$	$M=2$	-42.81	-52.63
	36	$K=2, N=3$	$M=3$	-43.28	-53.22
	72	$K=3, N=3$	$M=5$	-43.71	-53.05
Memory Binomial	28	$N=3$	$M=2$	-42.23	-51.45
	57	$N=4$	$M=3$	-43.52	-52.77
	121	$N=5$	$M=5$	-43.57	-52.85

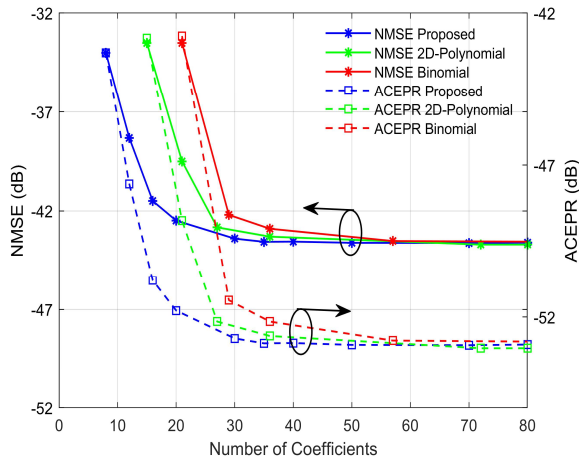


**Fig. 8.** NMSE (Solid lines) and ACEPR (dashed lines) versus the number of coefficients for the proposed model, dual-input memory polynomial model, and memory binomial model.

#### 4.3 Digital Predistortion Results

The proposed digital predistortion was evaluated in the time domain and in the frequency domain using WCDMA measurement data. The ET PA AM/AM and AM/PM conversions for both cases with and without DPD are shown in Fig. 9. The proposed DPD model clearly improved the ET PA linearity in both amplitude and phase characteristics. The DPD linearization capability in a frequency domain using the Power Spectral Density (PSD) is shown in Fig. 10. An improvement of -17.11/-16.75 dB in Adjacent Channel Power (ACPR) was observed in the PSD when the DPD was applied to compensate for the nonlinear distortion. Table 2 reports the ACPR values versus the number of coefficients for the proposed DPD model, and compared to the state-of-the-art 2D-polynomial and binomial models.

#### 5. Conclusions

This paper proposed a new behavioral model and digital predistortion for the envelope tracking RF power

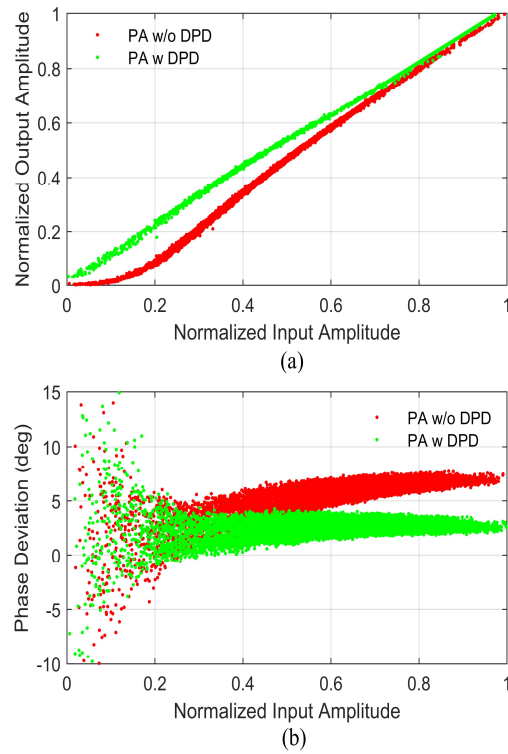


**Fig. 9.** The AM/AM and AM/PM conversions of the ET PA with and without DPD. (a) AM/AM conversion. (b) AM/PM conversion.

amplifiers. The proposed model characterizes the dynamic nonlinearity in the AM/AM and AM/PM conversions due to the hysteresis effects in the power amplifier circuits. The Hammerstein approach was applied to model the dynamic nonlinearity in the AM/PM conversion, since it can provide high accuracy at low complexity. The proposed model considers the nonlinearity effect due to the time-varying supply voltage in the envelope tracking case. Digital predistortion was derived to compensate for the nonlinear distortion in the AM/AM and AM/PM conversions. In addition the DPD model compensated for the nonlinearity

**Table 2** DPD model results in ACPR versus the number of coefficients

Case	Nonlinear Order	Number of Coefficients	ACPR (dBc) -/+4 MHz
PA Input	*	*	-65.85/-64.32
PA Output	*	*	-35.22/-34.56
Saleh DPD	*	4	-38.03/-36.82
Extended Saleh DPD	$N_A=2, N_B=4, P_a=2, P_b=3$	11	-51.28/-50.25
	$N_A=6, N_B=5, P_a=5, P_b=2$	18	-52.33/-51.31
Dual-Input Polynomial DPD	$K=2, N=5$	15	-50.05/-49.10
	$K=3, N=9$	36	-51.68/-50.59
Binomial DPD	$Q=5$	21	-49.71/-48.68
	$Q=7$	36	-51.25/-50.27

due to the dynamic supply voltage. The proposed ET PA model and DPD parameters can be calculated easily using a least squares method. The proposed model was evaluated using NMSE and ACEPR for different number of coefficients and memory depth. The optimal modeling accuracy was -42.48 dB in NMSE, and -51.8 dB in ACEPR. The proposed DPD linearization was evaluated in ACPR using WCDM signal. The obtained ACPR was -52.33/-51.31 dB for the ET PA with DPD, whereas it was -35.22/-34.56 dB for the ET PA without DPD. Our reported results showed how the proposed ET PA and DPD models can achieve such performance with a lower number of coefficients and a lower computational cost compared to the state-of-the-art dual-input memory polynomial and binomial models.

## References

- [1] Y. Xiong, C. Zhao, K. Kang, et al, "A high-efficiency supply modulator with a highly-linear envelope detector for WCDMA envelope-tracking applications," *AEU - International Journal of Electronics and Communications*, Vol. 70, no. 9, PP. 1350-1355, 2016.
- [2] Z. Wang, "Envelope Tracking Power Amplifiers for Wireless Communications," Artech House, USA, 2014.
- [3] J. Jeong, D. Kimball, M. Kwak, et al, "Wideband Envelope Tracking Power Amplifiers With Reduced Bandwidth Power Supply Waveforms and Adaptive Digital Predistortion Techniques," in *IEEE Transactions on Microwave Theory and Techniques*, vol. 57, no. 12, pp. 3307-3314, 2009.
- [4] J. Kim, S. Member, D. Kim, et al "Analysis of envelope tracking power amplifier using mathematical modeling," *IEEE Transactions on Microwave Theory and Techniques*, vol. 62, no. 6, pp. 1352-1362, 2014.
- [5] H. Al-kanan, F. Li, F. Tafuri, "Extended Saleh model for behavioral modeling of envelope tracking power amplifiers," 2017 IEEE 18th Wireless and Microwave Technology Conference (WAMICON), Cocoa Beach, FL, pp. 1-4, 2017.
- [6] F. Tafuri, D. Sira, T. Nielsen, et al, "Memory models for behavioral modeling and digital predistortion of envelope tracking power amplifiers", *Microprocessors and Microsystems*, vol. 39, no. 8, , pp. 879-888, 2015.
- [7] H. Al-Kanan, F. Li, F. Tafuri, "Comparison of 2-D Behavioral Models for Modeling and Digital Predistortion of Envelope Tracking Power Amplifiers," 2017 Asia-Pacific Microwave Conf. (APMC), Kuala Lumpur, pp. 1-4 , 2017.
- [8] F. Tafuri, T. Larsen, "Extended Cann model for behavioral modeling of envelope tracking power amplifiers," *ISPACS 2013 – 2013 Int. Symp. Intell. Signal Process. Commun. Syst.*, no. 4, pp. 670-673, 2013.
- [9] F. Taringou, O. Hammi, B. Srinivasan, et al, "Behaviour modeling of wideband RF transmitters using Hammerstein-Wiener models," in *IET Circuits, Devices & Systems*, vol. 4, no. 4, pp. 282-290, 2010.
- [10] A. Saleh, "Frequency independent and frequency dependent nonlinear model of TWT amplifiers," *IEEE Transaction on Communications*, vol. COM-29, pp. 1715-1720, 1981.
- [11] A. Hekkala, A. Kotelba, M. Lasanen, "Compensation of linear and nonlinear distortions in envelope tracking amplifier," 2008 IEEE 19th International Symposium on Personal Indoor and Mobile Radio Communications, Cannes, pp. 1-5, 2008.
- [12] H. Ku, M. McKinley, 'Quantifying memory effects in RF power amplifiers', *IEEE Transaction on Microwave Theory and Techniques*, Vol. 50, no. 12, pp. 2843-2849, 2002.
- [13] K. Moon, Y. Cho, J. Kim, et al, "Investigation of Intermodulation Distortion of Envelope Tracking Power Amplifier for Linearity Improvement", *IEEE Transaction on Microwave Theory and Techniques*, vol.63, no.4, 2015.
- [14] M. Shammasi, S. Safavi, "Performance of a predistorter based on Saleh model for OFDM systems in HPA nonlinearity," 2012 14th Int. Conf. Advanced Commun. Techn. (ICACT), pp. 148-152, 2012.
- [15] T. Nguyen, J. Yoh, C. Lee, et al, "Modeling of HPA

and HPA linearization through a predistorter: Global Broadcasting Service applications," in IEEE Transactions on Broadcasting, vol. 49, no. 2, pp. 132-141, 2003.

- [16] J. Wood, "Behavioral Modeling and Linearization of RF Power Amplifiers", Artech House, USA, 2014.

ACCEPTED MANUSCRIPT

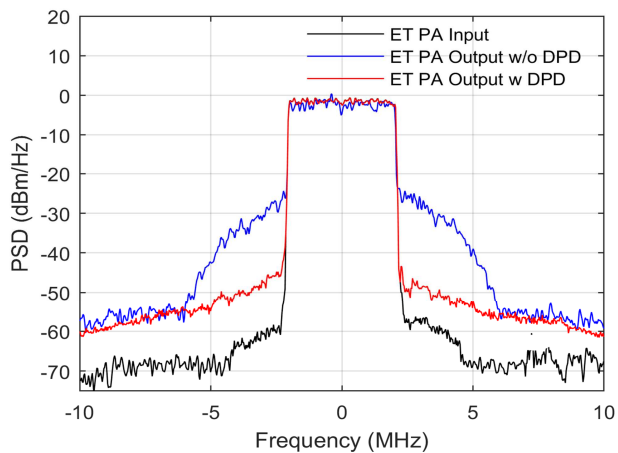


**Fig. 10.** Normalized Power Spectral Density (PSD) of the ET PA output with and without Digital Predistortion.

